CHEMICAL ENGINEERING TRANSACTIONS
VOL. 111, 2024
A publication of AIDIC
The Italian Association of Chemical Engineering
Online at www.cetjournal.it
Guest Editors: Valerio Cozzani, Bruno Fabiano, Genserik Reniers

ISBN 979-12-81206-11-3; **ISSN** 2283-9216
DOI: 10.3303/CET24111099

CO_2 Chemical Absorption with NH_3 in Bubble Column and Packed Bed System: Modeling and Experiments

Federico Atzori[a], Francesco Barzagli[b], Giacomo Cao[a,c,d], Alessandro Concas[a,c*]

[a]Department of Mechanical, Chemical and Materials Engineering, University of Cagliari, Piazza d'Armi, 09123 Cagliari, Italy
[b]National Research Council (CNR), ICCOM Institute, via Madonna del Piano 10, 50019 Sesto F.no, Florence, Italy
[c]Interdepartmental Center of Environmental Science and Engineering (CINSA), Via San Giorgio 12, 09124 Cagliari, Italy
[d]Center for Advanced Studies, Research and Development in Sardinia (CRS4), Piscina Manna, Building 1, 09050 Pula (CA), Italy
alessandro.concas@unica.it

The chemical absorption of CO_2 from a flue gas with aqueous NH_3 is investigated both experimentally and theoretically. An equilibrium-based approach is proposed to model the reactions between the dissolved CO_2 and NH_3 in the liquid phase. Such an approach was then integrated into two different sets of balance equations for packed bed and bubble column systems, respectively. To validate the models, two sets of experimental campaigns were carried out under different operating conditions. The good agreement between computational and experimental results confirmed the effectiveness of the models, whose results might be useful to properly design, optimize and control the CO_2 capture and the sorbent regeneration, whose energy demand depends on the chemical composition of the sorbent that can be suitably predicted by the developed models.

1. Introduction

One of the most critical challenges of the recent decades is to reduce greenhouse gas emissions and, in particular, CO_2 that accounts for 74 % of the total anthropogenic emissions. For this reason, carbon capture and utilization (CCU) technologies have been extensively studied in order to limit carbon emissions and use antropogenic CO_2 as a renewable feedstock, suitable in several applications, from fuel synthesis (Al-Mamoori et al., 2017) to photobioreactor (PBR) feed for microalgae growth (Concas et al., 2015). Moreover, CO_2 capture and utilization for microalgae growth has gained increasing interest for sustaining manned missions on Mars (Fais et al; 2022) where in situ resources, such as CO_2 and regolith, can be exploited to produce oxygen and food (Concas et al., 2023). According to chemical and petrochemical industries, chemical absorption is one of the most feasible methods for post combustion CO_2 capture and a mature technology ready to retrofit existing power plants (Ochedi et al., 2021). Due to the chemical reactions that consume the absorbed carbon dioxide, the capture capacity of the sorbent solution increases with respect to physical absorption, reducing the energy demand related to pressurization and cooling and allowing to purify flow gases with CO_2 concentration lower than 15 $\%_{vol}$ (Ochedi et al., 2021). Accordingly, the most significant challenge is to discover and test chemical solvents with high absorption capacity, low regeneration energy, good thermal degradation resistance and low volatility. Recently, ammonia (NH_3) has demonstrated to be one of the most promising solvents, due to its high absorption rate compared to traditional sorbents, like monoethanolamine (MEA), its cost-effectiveness, its low regeneration energy and its resistance to degradation in the presence of O_2 and SO_x (Puxty et al., 2010). Nevertheless, NH_3 high volatility must be suitably managed to permit large-scale implementations (Jilvero et al., 2014). In this work, a specific mathematical modelling approach, based on the limiting step theory and the steady-state assumption for the chemicals in the liquid phase, was developed and applied to describe the capture phenomenon within bubble columns. After model validation through a comparison with experimental data of capture efficiency and sorbent chemical composition, obtained with a lab-scale bubble column, the same modelling approach was used to write a model for simulating the capture process within packed columns, with the aim to implement a model-based algorithm for the column design, able to compute the column height, given

Paper Received: 6 February 2024; Revised: 27 April 2024; Accepted: 10 August 2024
Please cite this article as: Atzori F., Barzagli F., Cao G., Concas A., 2024, CO_2 Chemical Absorption with NH_3 in Bubble Column and Packed Bed System: Modeling and Experiments, Chemical Engineering Transactions, 111, 589-594 DOI:10.3303/CET24111099

the capture efficiency to be achieved. Finally, a lab-scale packed column was used to perform an experimental campaign that confirmed the effectiveness of the algorithm and the modelling approach.

2. Materials and method

Two different experimental campaigns were conducted to analyse the capture process both in bubble column and packed bed system, under isothermal condition, guaranteed by a thermostatic bath. The flue gas to be purified was composed by pure CO_2 and N_2, mixed together; the gas flow rate (Q_G) was regulated by means of digital gas mass flow controllers (Aalborg), equipped with gas flowmeters (Cole Parmer) and the CO_2 concentration in the gas mixture entering and exiting from the absorber was measured with a Varian CP-4900 gas chromatograph. The percentage of CO_2 in the outlet stream is continuously measured in order to calculate the capture efficiency, defined as the ratio between the absorbed and the inlet CO_2 (mol/s).

2.1 CO_2 capture experiment whit bubble column system

The CO_2 capture was performed in a home-built glass cylinder with a diameter of 56 mm and a height of 300 mm. The absorber was charged with 0.150 dm^3 of aqueous NH_3 solution and fitted with a sintered gas diffuser in the bottom. Measurements of solution pH were performed with a HI98128 pHep®5 pH & temperature tester (Hanna Instruments), while the identification and quantification of the species formed during the capture process was obtained with an accurate in continuous ^{13}C NMR analysis. A schematic representation of the apparatus is shown in Figure 1a, while a more detailed report about the experimental procedure can be found in Atzori (2023). To validate the model and verify its robustness, three different series of experiments were conducted, varying operational parameters such as the sorbent initial C_{NH_3} and the system temperature, as summarized in Table 1.

Table 1: Experimental operating conditions for CO_2 capture in bubble column

Exp	T [°C]	$C_{NH_3}^{in}$ [M]	Q_G [m^3/h]	$y_{CO_2}^{in}$ [%]
1	5	1	$12.2 \cdot 10^{-3}$	15
2	20	1	$12.2 \cdot 10^{-3}$	15
3	20	0.5	$12.2 \cdot 10^{-3}$	15

2.2 CO_2 capture experiment whit packed bed system

The absorber was a glass column (height 520 mm, internal diameter 40 mm), packed with glass rings (height 6 mm, internal diameter 4.5 mm, external diameter 6 mm, nominal size 6 mm), for a packing height of 400 mm. The experimental procedure is described in detail in Atzori (2024). Three different experimental trials were conducted in different operating conditions (Table 2) and repeated twice for the sake of reproducibility.

Table 2: Experimental operating conditions for CO_2 capture in packed bed system

Exp	T [°C]	$C_{NH_3}^{in}$ [M]	Q_G [m^3/h]	Q_L [m^3/h]	$y_{CO_2}^{in}$ [%]
4	10	1	$25.47 \cdot 10^{-3}$	$1.67 \cdot 10^{-3}$	10
5	0	1	$25.47 \cdot 10^{-3}$	$1.67 \cdot 10^{-3}$	10
6	0	2	$25.47 \cdot 10^{-3}$	$1.67 \cdot 10^{-3}$	10

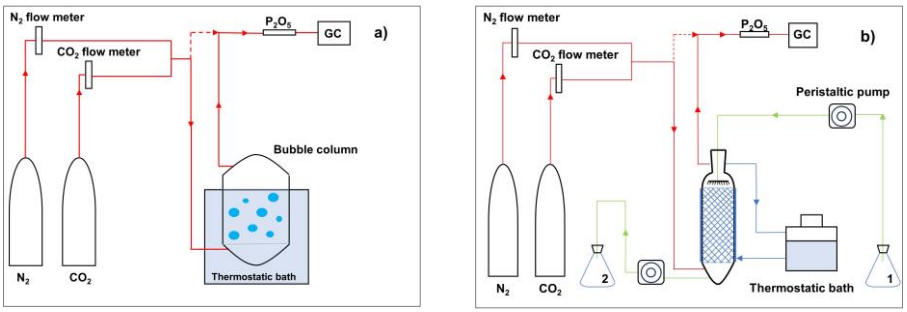

Figure 1: Experimental setup of CO_2 capture in bubble column (a) and packed bed system (b).

Each experimental trial was divided into 10 consecutive steps. Referring to Figure 1b, in the first step of each experiment, 400 mL of fresh ammonia solution was prepared and stored in flask 1. At the start of the step, such a solution was fed from the top of the column at the desired flow rate (Q_L), while, countercurrent to the NH_3

solution flow, the gaseous CO_2/N_2 mixture was fed from the bottom. After passing through the entire column, the CO_2-rich ammonia solution was stored in the flask 2. At the end of the first step, the solution stored in the flask 2 was transferred in the flask 1 and the second step begins. The same procedure was adopted for a total of 10 subsequent steps. The absorption efficiency and the total amount of captured CO_2 were measured for each operating step. Every experimental trial was repeated twice for the sake of reproducibility.

3. Model

In this section the models developed for bubble column and packed bed system are parallelly described.
Based on the rate-based approach, both models consider two different control volumes, the gas and the liquid phase, physically interconnected by the gas–liquid interface (Ramesh et al., 2007). The mass transfer of CO_2 (absorbed) and NH_3 (evaporated) was rigorously modelled by means of two film theory (Whitman, 1923), as expressed with Eq(1) and Eq(2), used for bubble column and packed bed, respectively.

$$J_i^{bc} = \varepsilon_i \cdot K_{L,i}\left(\frac{p_i}{H_i} - C_i\right) \tag{1}$$

$$J_i^{pb} = K_{G,i}(p_i - H_i \cdot C_i) \tag{2}$$

The expression to evaluate Henry constants (H_i) and overall transfer coefficient for gas ($K_{G,i}$) and liquid phase ($K_{L,i}$) were inferred from Sanders (2015) and Perry (1950), respectively. The strategy adopted to simulate the bubble column unsteady state operation relies on the classical homogeneous model for unstirred tank reactors, operated continuously for the gas phase and in batch mode for the liquid one; Therefore, the gas phase material balance for the ith species was written as expressed in Eq(3)

$$\frac{dp_i}{dt} = \frac{R \cdot T}{V_G}\left(N^{in} \cdot y_i^{in} - S \cdot J_i^{bc} - N^{out} \cdot y_i\right). \qquad p_i(t=0) = p^0{}_i \tag{3}$$

The equations for the packed bed steady-state operation can be developed, by considering the following assumptions: the liquid solution is ideal and incompressible; the liquid and gas phases properties are constant along the radial direction; there is no axial dispersion and the volumetric flow rates are constant; liquid and gas interstitial velocity are zero along the radial direction; liquid and gas velocity field are assumed to be uniform along the column. Accordingly, considering the spatial domain direction going from the bottom (z = 0), to the top of the column (z = Z), the gas phase balance for the ith species was written as reported in Eq(4).

$$\frac{dp_i}{dz} = -\frac{R \cdot T}{v_G \cdot \zeta_G} \cdot a_w \cdot J_i^{pb} \qquad p_i(z=0) = p^{in}{}_i \tag{4}$$

Once the CO_2 is absorbed, it reacts with water and NH_3, following the reaction scheme reported in Table 3.

Table 3. Chemical reactions

Reaction	ID
$CO_2 + H_2O \overset{K_1}{\Leftrightarrow} HCO_3^- + H^+$	R.1
$HCO_3^- \overset{K_2}{\Leftrightarrow} CO_3^{2-} + H^+$	R.2
$2NH_3 + CO_2 \overset{K_3}{\Leftrightarrow} NH_2CO_2^- + NH_4^+$	R.3
$NH_3 + HCO_3^- \overset{K_4}{\Leftrightarrow} NH_2CO_2^- + H_2O$	R.4
$NH_3 + H_2O \overset{K_{am}}{\Longleftrightarrow} NH_4^+ + OH^-$	R.5
$H_2O \overset{K_W}{\Leftrightarrow} OH^- + H^+$	R.6

Referring to (R.1-R.6), total carbon (C_t) and total nitrogen (N_t) speciation was expressed via Eq(5) and Eq(6).

$$C_{Ct} = C_{CO_2} + C_{HCO_3^-} + C_{CO_3^{2-}} + C_{NH_2CO_2^-} \tag{5}$$

$$C_{Nt} = C_{NH_3} + C_{NH_4^+} + C_{NH_2CO_2^-}\ , \tag{6}$$

while the solution electroneutrality was taken into account with Eq(7)

$$\mathrm{E}_L = 0 = C_{H^+} - C_{OH^-} - C_{HCO_3^-} - 2C_{CO_3^{2-}} - C_{NH_2CO_2^-} + C_{NH_4^+}. \tag{7}$$

Since CO_2 absorption and NH_3 evaporation are the only interface transfer processes, the molar balances of C_t and N_t could be written with Eq(8) and Eq(9), for bubble column and with Eq(10) and Eq(11), for packed bed

$$\frac{d(C_{C_t})}{dt} = \frac{S}{V_L} \cdot J_{CO_2}^{bc} \tag{8}$$

$$\frac{d(C_{N_t})}{dt} = \frac{S}{V_L} \cdot J_{NH_3}^{bc} \tag{9}$$

$$\frac{d(C_{C_t})}{dz} = -\frac{a_w}{v_L \zeta_L} \cdot J_{CO_2}{}^{pb} \tag{10}$$

$$\frac{d(C_{N_t})}{dz} = -\frac{a_w}{v_L \zeta_L} \cdot J_{NH_3}{}^{pb} \ . \tag{11}$$

Since the interface mass transfer is the rate limiting-step, the steady-state approximation could be used to describe the reaction dynamics and, as a consequence, the species concentration into the liquid phase could be related by means of the thermodynamical equilibrium relations, as shown in Eq(12-14) (Atzori et al., 2024).

$$C_{C_t} = C_{CO_2} + \frac{K_1 C_{CO_2}}{C_{H^+}} + \frac{K_1 K_2 C_{CO_2}}{C_{H^+}{}^2} + \frac{K_3 K_w C_{CO_2} C_{NH_3}}{C_{H^+} C_{H2O} K_{am}} \tag{12}$$

$$C_{N_t} = C_{NH_3} + \frac{K_{am} C_{NH_3} C_{H2O} C_{H^+}}{K_w} + \frac{K_3 K_w C_{CO_2} C_{NH_3}}{C_{H^+} C_{H2O} K_{am}} \tag{13}$$

$$\mathrm{E}_L = 0 = C_{H^+} - \frac{K_w}{C_{H^+}} - \frac{K_1 C_{CO_2}}{C_{H^+}} - 2\frac{K_1 K_2 C_{CO_2}}{C_{H^+}{}^2} - \frac{K_3 K_w C_{CO_2} C_{NH_3}}{C_{H^+} C_{H2O} K_{am}} + \frac{K_{am} C_{NH_3} C_{H2O} C_{H^+}}{K_w} \tag{14}$$

Let φ be the independent variable, either t or z, depending on the specific model being developed; the previous equations were derived with respect to φ and, using the chain rule, Eq. (15-17) were obtained

$$\frac{dC_{C_t}}{d\varphi} = \frac{\partial C_{C_t}}{\partial C_{CO_2}} \frac{dC_{CO_2}}{d\varphi} + \frac{\partial C_{C_t}}{\partial C_{NH_3}} \frac{dC_{NH_3}}{d\varphi} + \frac{\partial C_{C_t}}{\partial C_{H^+}} \frac{dC_{H^+}}{d\varphi} \tag{15}$$

$$\frac{dC_{N_t}}{d\varphi} = \frac{\partial C_{N_t}}{\partial C_{CO_2}} \frac{dC_{CO_2}}{d\varphi} + \frac{\partial C_{N_t}}{\partial C_{NH_3}} \frac{dC_{NH_3}}{d\varphi} + \frac{\partial C_{N_t}}{\partial C_{H^+}} \frac{dC_{H^+}}{d\varphi} \tag{16}$$

$$\frac{dC_{E_L}}{d\varphi} = 0 = \frac{\partial C_{E_L}}{\partial C_{CO_2}} \frac{dC_{CO_2}}{d\varphi} + \frac{\partial C_{E_L}}{\partial C_{NH_3}} \frac{dC_{NH_3}}{d\varphi} + \frac{\partial C_{E_L}}{\partial C_{H^+}} \frac{dC_{H^+}}{d\varphi} \tag{17}$$

Eq(15-17) were seen as an algebraic equation system whose unknown are $d(C_{CO_2})/d(\varphi)$, $d(C_{NH_3})/d(\varphi)$, and $d(C_{H^+})/d(\varphi)$. Note that the partial derivatives of C_t, N_t and E_L are functions of C_{CO_2}, C_{NH_3} and C_{H^+} and that the total derivatives of C_{C_t} can be expressed with respect to C_{CO_2} and p_{CO_2}, by Eq(8) or Eq(10), as well as the partial derivatives of C_{N_t} can be written as a function of C_{NH_3} and p_{NH_3}, by Eq(9) or Eq(11). By solving Eq(15-17), the right-hand side of Eq(18-20) were found, as a function of C_i and p_i. For the sake of simplicity, it is reported in the form of generic functions f. Finally, to mathematically close the model, Eq(18-20) needed to consider the gas phase molar balances, given by Eq(3) for bubble column and Eq(4) for packed bed model.

$$\frac{dC_{CO_2}}{d\varphi} = f_1(C_{CO_2}, C_{NH_3}, C_{H^+}, p_{CO_2}, p_{NH_3}) \qquad \varphi \equiv t, C_{CO_2}|_{t=0} = C^0{}_{CO_2}; \quad \varphi \equiv z, C_{CO_2}|_{z=Z} = C^{in}{}_{CO_2} \tag{18}$$

$$\frac{dC_{NH_3}}{d\varphi} = f_2(C_{CO_2}, C_{NH_3}, C_{H^+}, p_{CO_2}, p_{NH_3}) \qquad \varphi \equiv t, C_{NH_3}|_{t=0} = C^0{}_{NH_3}; \quad \varphi \equiv z, C_{NH_3}|_{z=Z} = C^{in}{}_{NH_3} \tag{19}$$

$$\frac{dC_{H^+}}{d\varphi} = f_3(C_{CO_2}, C_{NH_3}, C_{H^+}, p_{CO_2}, p_{NH_3}) \qquad \varphi \equiv t, \ C_{H^+}|_{t=0} = C^0{}_{H^+}; \quad \varphi \equiv z, C_{H^+}|_{z=Z} = C^{in}{}_{H^+} \tag{20}$$

Once the C_{CO_2}, C_{NH_3} and C_{H^+} profiles were computed via eq. (18-20) the equilibrium relations of (R.1-R.6) can be used to compute the concentration profile of any other species.

4. Results

The bubble column model accuracy was evaluated by comparing the experimental measurements of capture efficiency (η), ion speciation and sorbent solution pH to the corresponding model results. Figure 2 shows the capture efficiency experimental data of Exp.1-3 and the corresponding model predictions that turned out to be able to grasp the efficiency dynamics, both in the first phase, when the high driving force led to efficiency values close to unity, and in the efficiency decrease phase, due to ammonia consumption and CO_2 accumulation in the sorbent solution. The offset that characterizes the curves in Figure 2a-b is probably due to an additional reactive phenomenon not accounted for, which becomes relevant when C_{NH3} is extremely low: H_2O substitutes one of

the two NH_3 molecules in R.3, thus limiting CO_2 accumulation in the final step of the process. In Exp. 3, the low initial NH_3 concentration led to its complete consumption in the early phase and hindered to visualize this phenomenon. However, the potential implication of such an offset should not be relevant in view of the transposition of the obtained results to the operative scale.

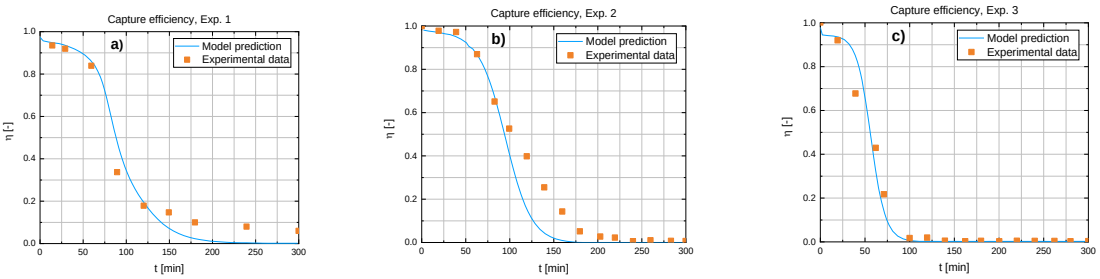

Figure 2: Capture efficiency in Exp. 1 (a) MSE = 0.044, Exp. 2 (b) MSE = 0.003 and Exp. 3 (c) MSE = 0.003.

Figure 3 displays the experimental results of the sorbent solution chemical composition and the corresponding model simulation, showing a good agreement between model and experimental results. Initially, the strong alkalinity of the solution promoted CO_3^{2-} production; however, the absorbed CO_2 led to a pH decrease, that slowed down the CO_3^{2-} formation to the advantage of HCO_3^- and $NH_2CO_2^-$. Evidently, the $NH_2CO_2^-$ profile was affected by NH_3 concentration, whose consumption determined the $NH_2CO_2^-$ synthesis stop.

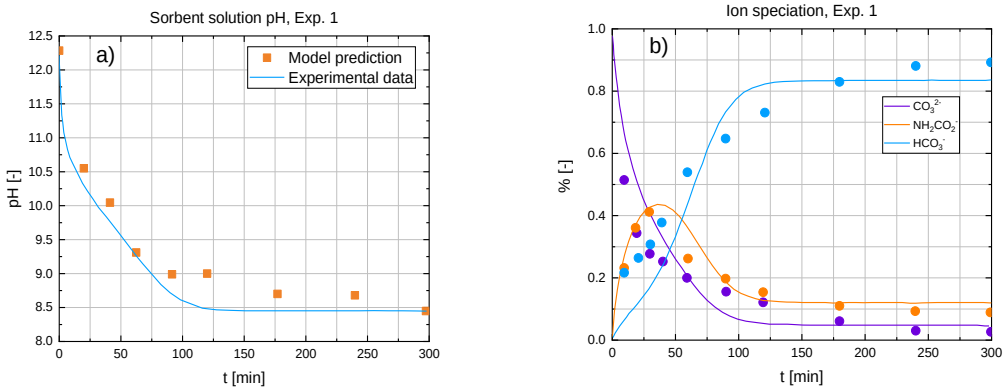

Figure 3: Sorbent solution pH (a) MSE = 0.009 and ion speciation (b) MSE = 0.007, in Exp. 1.

The effectiveness and the accuracy of the bubble column model simulations, led to consider the same thermodynamical assumptions to develop the packed bed model equations that were in turn used to implement the algorithm for the column height calculation (Z), as a function of the operating conditions (temperature and inlet composition) and the capture specification, namely the efficiency (η).
For every step of Exp. 4-6, η was measured and the algorithm was used to evaluate Z for achieving the desired η. Figure 4 shows two series of calculated values since η measurements were repeated twice for every trial. The capture device had a defined height (4 dm) that, consequently, was the value the calculation should provide. In Figure 4 the design algorithm results are reported showing a good approximation of the actual height of the capture device for the three experimental trials, despite the variation of operating conditions.

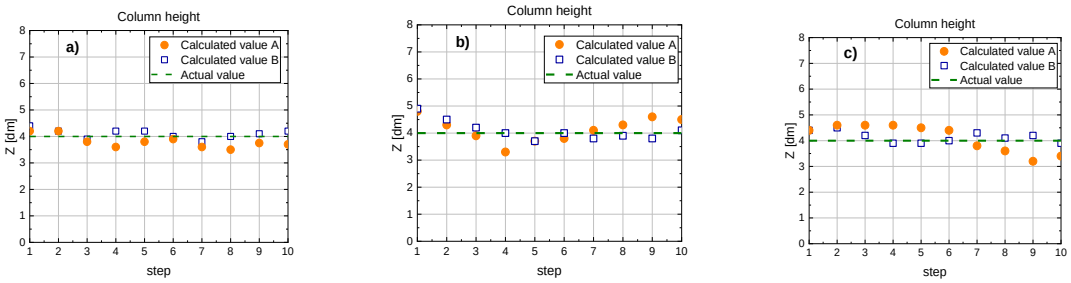

Figure 4: Column height evaluation in Exp. 4 (a) MSE = 0.064, Exp. 5 (b) MSE = 0.176, Exp. 6 (c) MSE = 0.224

5. Conclusions

In this work, the CO_2 chemical absorption in NH_3 solution was studied. An equilibrium-based approach was developed to account for nitrogen and carbon speciation into the sorbent solution and write an accurate mathematical model for the simulation of unsteady-state bubble column operation. The model equations managed to determine the time profile of the capture efficiency and sorbent solution chemical composition with a good accuracy compared to experimental results, obtained with a lab-scale bubble column, for different operating conditions. A model to simulate the steady-state operation of packed bed columns was then written and used to implement a design algorithm for the column height determination. Experimental trials were performed on a lab-scale packed column where the capture efficiency was measured to be used as input in the design algorithm that turned out to be able to approximate the actual height of the capture device.

Nomenclature

a_w – Wetted area per unit volume, m^2/m^3
C_i – i^{th} species liquid phase concentration, mol/m^3
H_i – i^{th} species Henry constant, $(Pa \cdot m^3)/mol$
J_i – i^{th} species molar flux, $mol/(s \cdot m^2)$
$K_{G(L),i}$ – Gas (liquid) overall transfer coefficient, $mol/(Pa \cdot s \cdot m^2)$, (m/s)
N – Molar flow rate, mol/s
p_i – i^{th} species gas phase partial pressure, Pa
R – Gas constant, J/(mol·K)
S – gas-liquid transfer interface, m^2
t – Time, s
T – Temperature, °C
$v_{G(L)}$ – Interstitial gas (liquid) velocity, m/s
$V_{G(L)}$ – Gas (liquid) phase volume, m^3
y_i – i^{th} species gas phase molar fraction, -
z – Spatial coordinate, m
ε_i – Enhancement factor, -
$\zeta_{G(L)}$ – Gas (liquid) volume fraction, -

Acknowledgments

F.A performed his activity in the framework of the PhD in Innovation Sciences and Technologies at the University of Cagliari, Italy. This work has been developed within the framework of the project eINS-Ecosystem of Innovation for Next Generation Sardinia (cod. ECS 00000038) funded by the Italian Ministry for Research and Education (MUR) under the National Recovery and Resilience Plan (PNRR) - MISSION 4 COMPONENT 2, "From research to business" INVESTMENT 1.5, "Creation and strengthening of Ecosystems of innovation" and construction of "Territorial R&D Leaders".

References

Al-Mamoori A., Krishnamurthy A., Rownaghi A. A., Rezaei F., 2017, Carbon capture and utilization update, Energy Technology, 5(6), 834-849.
Atzori F., Barzagli F., Varone A., Cao G., Concas A., 2023, CO2 absorption in aqueous NH3 solutions: Novel dynamic modeling of experimental outcomes, Chemical Engineering Journal, 451, 138999.
Atzori F., Barzagli F., Dai S., Concas A., Cao G., 2024, A new model-aided approach for the design of packed columns for CO2 absorption in aqueous NH3 solutions, Chemical Engineering Science, 2024, 119780.
Concas A., Pisu M. and Cao G., 2015, Microalgal cell disruption through Fenton reaction: experiments, modeling and remarks on its effect on the extracted lipids composition, Chemical Engineering Transactions, 43, 367-373.
Concas A., Fais G., Enna M., Zucchelli S., Caboni P., Lai N., Cincotti A., Cao, G., 2023, Modeling and experimental assessment of Synechococcus nidulans cultivation using simulated Martian medium and astronauts' urine,Acta Astronautica, 205, 185-198.
Fais G., Manca A., Concas A., Pantaleo A., Cao G., 2022, A novel process to grow edible microalgae on Mars by exploiting in situ-available resources: Experimental investigation. Acta Astronautica, 201, 454-463.
Jilvero H., Normann F., Andersson K., Johnsson F., 2014, The Rate of CO2 Absorption in Ammonia-Implications on Absorber Design, Industrial & Engineering Chemistry Research, 53(16), 6750-6758.
Ochedi F.O., Yu J., Yu H., Liu Y., Hussain A., 2021, Carbon dioxide capture using liquid absorption methods: a review, Environmental Chemistry Letters, 19, 77-109.
Perry, J. H. (1950). Chemical engineers' handbook, ACS Publications.
Puxty G., Robert R., Moetaz A., 2010, Comparison of the rate of CO2 absorption into aqueous ammonia and monoethanolamine, Chemical Engineering Science,65 (2), 915-922.
Ramesh K., Aziz N., Abd Shukor S. R., Ramasamy, M., 2007, Dynamic rate-based and equilibrium model approaches for continuous tray distillation column, Journal of Applied Sciences Research, 3(12), 2030-2041.
Sander R., Compilation of Henry's law constants (version 4.0) for water as solvent, 2015, Atmospheric Chemistry and Physics, 15, 4399–4981.
Whiteman, W. G., 1962, The two-film theory of gas absorption, International Journal of Heat and Mass Transfer, 5 (5) 429-433.